Adipocyte Pseudohypoxia Suppresses Lipolysis and Facilitates Benign Adipose Tissue Expansion

American Diabetes Association. diabetes

Adipocyte Pseudohypoxia Suppresses Lipolysis and Facilitates Benign Adipose Tissue Expansion

Journal:	*Diabetes*
Manuscript ID:	DB14-0233.R2
Manuscript Type:	Original Article
Date Submitted by the Author:	01-Sep-2014
Complete List of Authors:	MICHAILIDOU, ZOI; university of edinburgh, centre for cardiovascular research morton, nicholas; university of edinburgh, Moreno Navarrete, José Maria; Biomedical Research Institute of Girona, west, Christopher; university of edinburgh, Stewart, Kenneth; NHS SCOTLAND, Fernández-Real, José Manuel; Biomedical Research Institute of Girona, Schofield, Christopher; university of oxford, Seckl, Jonathan; university of edinburgh, Ratcliffe, Peter; university of oxford,

Adipocyte Pseudohypoxia Suppresses Lipolysis and Facilitates Benign Adipose Tissue Expansion

Zoi Michailidou [1,2*], Nicholas M Morton [2], José Maria Moreno Navarrete[3], Christopher C West[4], Kenneth J Stewart[5], José Manuel Fernández-Real[3], Christopher J Schofield[6], Jonathan R Seckl[2], Peter J Ratcliffe[1]

Author Affiliation:

[1] Henry Wellcome Building for Molecular Physiology, University of Oxford, Roosevelt Drive, Oxford OX3 7BN [2] The University of Edinburgh /BHF Centre for Cardiovascular Science, Queen's Medical Research Institute, 47 Little France Crescent, Edinburgh EH16 4TJ, [3]Biomedical Research Institute of Girona (IDIBGI), [4] The University of Edinburgh/MRC Centre for Regenerative Medicine, [5]The Department of Plastic, Reconstructive and Burns Surgery, St Johns Hospital, Livingston, UK, [6] Chemistry Research Laboratory, Oxford University, Oxford OX1 3TA.

[*]**Corresponding author:** Michailidou Z, v1zmicha@staffmail.ed.ac.uk. Tel +44(0)131 2426720

Short title: "Pseudohypoxia" Supresses Adipocyte Lipolysis

Key words: hypoxia, adipose, fatty acids, vasculature, lipolysis

Prolyl hydroxylase enzymes (PHDs) sense cellular oxygen upstream of hypoxia-inducible factor (HIF) signalling leading to HIF degradation in normoxic conditions. Here we demonstrate that adipose PHD2 inhibition plays a key role in the suppression of adipocyte lipolysis. Adipose *Phd2* gene ablation in mice enhanced adiposity, with a parallel increase in adipose vascularization associated with reduced circulating non-esterified fatty acid (NEFA) levels and normal glucose homeostasis. *Phd2* gene-depleted adipocytes exhibited lower basal lipolysis in normoxia and reduced β-adrenergic-stimulated lipolysis in both normoxia and hypoxia. A selective PHD inhibitor suppressed lipolysis in murine and human adipocytes *in vitro* and *in vivo* in mice. PHD2 genetic ablation and pharmacological inhibition attenuated protein levels of the key lipolytic effectors hormone-sensitive lipase and adipose triglyceride lipase (ATGL), suggesting a link between adipocyte oxygen sensing and fatty acid release. *PHD2* mRNA levels correlated positively with mRNA levels of AB-hydrolase domain containing-5 (*ABHD5*), an activator of ATGL, and negatively with mRNA levels of lipid droplet proteins, perilipin and TIP47 in human subcutaneous adipose tissue. Therapeutic "pseudohypoxia" caused by PHD2 inhibition in adipocytes blunts lipolysis and promotes benign adipose tissue expansion and may have therapeutic applications in obesity or lipodystrophy.

In obesity, the gradual expansion of adipose tissue associates with local hypoxia due to an inadequate vascular response (1-2). Hypoxic adipose tissue, as found in diet-induced obesity models, or transgenic HIF-1α overexpression in adipose tissue associates with local inflammation, fibrosis and metabolic dysfunction (1-6). In contrast, in models of dietary obesity in which adipose tissue hypoxia is attenuated (11β-HSD1 deficient mice, transgenic adipose overexpression of VEGF), the structural and metabolic abnormalities are ameliorated and benign adipose tissue expansion occurs (7-10). Understanding mechanisms that allow benign expansion of adipose depots is of high importance as it may lead to therapeutic strategies for minimising the pathogenesis of obesity and/or lipodystrophy syndromes.

Critical for benign expansion of fat depots is efficient storage and release of fatty acids in adipocytes (11-12) and adequate expandability of the adipose-vascular network (13). Adipose tissue expansion is a dynamic process that involves adipocyte hypertrophy in combination with vascular re-modelling involving endothelial cells, macrophages and the extracellular matrix (13-16). Low oxygen tension (hypoxia) can occur due to an inability of the tissue to provide adequate compensatory vascular supply (1-5). In this context, cells respond to hypoxia by activation and stabilization of the hypoxia inducible factor alpha isoforms (HIFα) (17). Increased HIF-1α activation may contribute to the pathological changes within adipose tissue in obesity (1-5) in part through inhibition of peroxisome proliferator-activated receptor gamma-2 (PPARg2)-dependent adipogenesis (18). This concept is supported by the phenotype of transgenic mice overexpressing *Hif1a* in adipose tissue which exhibit insulin resistance and localised adipose tissue fibrosis (6). In contrast, HIF-2α promotes adipose differentiation *in vitro* and, given that HIF-2α levels are also increased after 4 weeks in high fat fed mice (19), may counter-act pathogenic changes associated with HIF-1 at early stages of obesity development. The oxygen sensitive signal event that regulates HIF is mediated by

hydroxylase enzymes that regulate the protein stability and consequent transcriptional activity of HIFα (20). HIF-prolyl hydroxylases (PHDs otherwise known as EGLNs) belong to the large family of Fe (II) and 2-oxoglutarate dependent oxygenases (21-24). PHDs hydroxylate conserved prolyl residues of the HIF1α and HIF2α subunits, thus promoting their binding to the von Hippel Lindau (VHL) tumor suppressor protein, which targets HIFα isoforms for proteasomal degradation in normoxia (21-24). In humans there are three isoforms of PHD enzymes (PHD1-3), with PHD2 (EGLN1) the most abundant enzyme, including in mature adipocytes (25). PHD2 is the most important for setting basal activity of the HIF system in most cells (20). Despite the growing understanding of the pathological role of HIF1α activation in adipose tissue during obesity (1-10, 26-32), direct pharmacological targeting of HIF remains challenging. In contrast, therapeutic targeting of PHDs to induce a "pseudohypoxic" (activation of HIF-α and target genes in normoxia) state is under active clinical development in the context of anemia, and other diseases involving hypoxia (33-34). Here we addressed the metabolic consequences and potential therapeutic impact of "pseudohypoxia" by genetic and pharmacological inhibition of the principal oxygen sensing enzyme PHD2 in adipose tissue.

RESEARCH DESIGN AND METHODS

Animal Studies. The *Phd2* conditional allele (35) on a congenic C57BL/6 background, the *Hif1a* conditional allele (36) and the *Hif2a* conditional allele (37) were crossed with the fatty acid binding protein 4 (*Fapb4*)-*Cre* allele (38, the Jackson Laboratories) to achieve adipose-specific conditional knockout mice. Hif1a (stock number 007561) and Hif2a (stock number 008407) mice were purchased from the Jackson Laboratories. Genotyping and recombination efficiency PCRs were performed as previously described (35-39). In all experiments described, control littermates were used for comparisons. For diet induced obesity experiments, mice were given the D12331 high fat diet (58% kcal fat; Research Diets Inc) for 12 weeks. To assess the effect on adipocyte lipolysis of pharmacologically inhibiting PHD, we used 2-(1-chloro-4-hydroxyisoquinoline-3-carboxamido) acetic acid (40-41), a potent small molecule inhibitor of the PHD enzymes that has been shown to activate HIFα (40-41). For analysis of the effects of this PHD inhibitor (PHI) *in vivo*, C57BL/6J mice were used. In brief, mice were fasted overnight, blood was collected for basal NEFA quantification, mice were then divided into 2 groups, those receiving intraperitonal (i.p.) PHI (30mg/kg; a dose that was sufficient to robustly induce HIF in liver (41) and a control group receiving vehicle (5% DMSO) alone. PHI was administered for an hour prior to CL316,243 (1µg/kg) stimulation. Male adult mice were used in all the experiments. Animals were bred under standard conditions and fed standard chow (product 801151; Special Diet Services, Essex, U.K.) *ad libitum* unless stated otherwise. Animal studies were performed under licensed approval in accordance with the U.K. Home Office Animals (Scientific Procedures) Act, 1986.

Systemic Tests and Biochemistry. For glucose tolerance tests mice were fasted 5h before administration of glucose (2mg/g BW) orally or by intraperitoneal (i.p) injection. Glucose concentration was measured by a blood glucose monitoring system (OneTouchUltra2,

Lifescan, Milpitas). For β-3 adrenergic receptor agonist tests, mice were fasted overnight and blood samples were collected before and 15, 30 and 60min after i.p. injection of 1μg/kg CL316,243 (Sigma-Aldrich, Dorset, U.K.). In the PHD inhibitor experiments, PHI was administered i.p. (30mg/kg) and blood collected one hour prior to the i.p. CL316,243 challenge. Insulin and leptin concentrations were measured using commercial Elisa kits (Crystal Chem Inc, Downers Grove). Liver and muscle triglyceride levels were measured using a commercial kit (Abcam, Cambridge, U.K.) according to the manufacturer's instructions.

RT-qPCR. Total RNA was extracted from cells and tissue using TRIZOL (Invitrogen, Paisley, U.K.) and treated with DNase I (Invitrogen, Paisley, U.K.). 1 μg total RNA was used for first-strand DNA synthesis using Superscript III cDNA Synthesis system (Invitrogen, Paisley, U.K.), and qPCR was performed with the Lightcycler 480 (Roche), using mouse-Taqman assays (Life technologies, Paisley, U.K.) for all genes measured. A standard curve was constructed for each gene measured using a serial dilution of cDNA pooled from all samples. Results were normalized to the expression of 18S rRNA.

Immunoblot Assays. Whole cell lysates were prepared in ice-cold buffer (5 mmol/L HEPES, 137 mmol/L NaCl, 1 mmol/L $MgCl_2$, 1 mmol/L $CaCl_2$, 10 mmol/L NaF, 2 mmol/L EDTA, 10 mmol/L Na pyrophosphate, 2 mmol/L Na_3VO_4, 1% Nonidet P-40, and 10% glycerol) containing protease inhibitors (Complete Mini; Roche Diagnostics Ltd., West Sussex, U.K.) Blots were probed with HIF-1α (Cayman, Ann Arbor, Michigan), HIF2-α (Novus Biologicals, Littleton), HIF Prolyl Hydroxylase 2 (Novus Biologicals, Littleton) antibodies. Lipolysis activation antibody kit was used to identify HSL, p-HSL660, p-HSL565 and perilipin (NE Biolabs, Ipswich). The ATGL, AKT and phospho-AKT (Ser473) antibodies were from Cell Signaling (Hertfordshire, U.K). HRP-conjugated anti-rabbit (Dako, Cambridgeshire, U.K.) secondary antibody was used. Signal was detected using ECL

Plus (GE Healthcare Life Sciences, Buckinghamshire, U.K.). Blots were re-probed with an HRP-conjugated anti-actin antibody (Abcam, Cambridge, U.K.). Densitometry was performed using the Image J software.

Histology and Immunohistochemistry. Formalin-fixed, paraffin embedded adipose sections (4μm) were used. Images were acquired using a Zeiss microscope (Welwyn Garden City, Hertfordshire, U.K.) equipped with a Kodak DCS330 camera (Eastman Kodak, Rochester, NY). Adipocyte size was calculated by measuring the diameter of adipocytes from 20 randomly selected areas per section using a Zeiss KS300 image analyser. Antibodies to CD31 (Abcam, Cambridge, U.K) for endothelial cells/vessels or F4/80 (Abcam, Cambridge, U.K) for macrophages were used. Binding of primary antibody was visualized using DAB, Chromogen-A (Dako, Cambridgeshire, U.K). Counter stain was performed by rinsing in 70% hematoxilin. Picrosirius red (Sigma Aldrich, Dorset, U.K.) staining of adipose sections was used to identify total collagen. Analysis was performed blind to the experimental grouping as previously described (7).

In vitro Adipocyte Lipolysis Experiments. Primary murine or human adipocytes were isolated as previously described (7). For the analysis of lipolysis in aP2-*Phd2*KO, aP2-*Hif1a*KO and aP2-*Hif2a*KO adipocytes, hypoxic stimulation was performed by replacing the media with 1% O_2 pre-conditioned media. Cells were left at 1% O_2 in a hypoxic chamber (1% O_2) for 4h, after which media was collected for measurement of NEFA release and cells were lysed in RIPA protein lysis buffer for analysis by immunoblotting. Effects of PHI on lipolysis were examined in C57BL/6J primary adipocytes. In brief, adipocytes were pre-treated with PHI (0.5mM, a sufficient dose to robustly activate HIFα (41) or vehicle (DMSO, 0.5%) for one hour prior to β-adrenergic stimulation with CL316,243 (100nM) for three hours. Medium was collected for measuring NEFA concentrations with a NEFA kit (Alpha

Labs, Eastleigh, U.K.) and adipocytes were lysed for protein quantification and immunoblot analysis.

Human Adipocyte Lipolysis Studies. Human abdominal subcutaneous adipose tissue was obtained, after written consent, from healthy female subjects (age range 30-50years old) with mean BMI 25.6 (±1.9 kg/m^2) undergoing cosmetic lipectomy procedures. Ethical approval for the collection of tissue and subsequent research was granted by the South East Scotland Research Ethics Committee 3 (SESREC03), reference number 10/S1103/45. Adipocytes were isolated as above and exposed to PHI as above. In brief, human adipocytes were pretreated with PHI or vehicle one hour prior to stimulation with isoproterenol (100nM) for additional two hours. Medium was collected for measuring NEFA concentrations and adipocytes were lysed for protein quantification and immunoblot analysis.

Human Adipose Tissue Gene Expression Study. Adipose tissue samples (91 subcutaneous and 102 omental abdominal) were obtained from the same location during elective surgical procedures [cholecystectomy (n=10), surgery of abdominal hernia (n=14) and gastric by-pass surgery (n=78)] from participants with BMI within 20- 68 kg/m^2. All subjects were of Caucasian origin and reported that their body weight had been stable for at least three months before the study. In the obese type 2 diabetic group, 2 subjects were treated with metformin, 1 with glitazones and 1 with insulin. Liver and renal diseases were specifically excluded by biochemical work-up, measuring biomarkers of liver and renal injury. All subjects gave written informed consent, approved by the ethical committee (Comitè d'Ètica d'Investigació Clínica, CEIC). Adipose tissue samples were immediately frozen in liquid nitrogen and stored at -80ºC. RNA was prepared using RNeasy Lipid Tissue Mini Kit (QIAgen,Izasa SA, Barcelona, Spain) and integrity checked by Agilent Bioanalyzer (Agilent Technologies, Palo Alto, CA) and reverse transcribed to cDNA using High Capacity cDNA Archive Kit (Applied Biosystems Inc, Madrid, Spain) according to the manufacturer's protocol. Gene expression

was assessed by real time PCR using a LightCycler® 480 Real-Time PCR System (Roche Diagnostics SL, Barcelona, Spain), using commercially available TaqMan® primer/probe sets (Applied Biosystems Inc, Madrid, Spain). A threshold cycle (Ct value) was obtained for each amplification curve and a ΔCt value was first calculated by subtracting the Ct value for human *Cyclophilin A* (PPIA) RNA from the Ct value for each sample. Fold changes compared with the endogenous control were then determined by calculating $2^{-\Delta Ct}$. Results are expressed as ratio to PPIA gene expression.

Statistics. Values are reported as mean±SEM. All statistical analysis was performed in GraphPad Prism 5 software. Simple comparisons were analysed using Student's *t* test. For multiple comparisons, differences between genotypes and the effect of treatment(s) were analysed by two-way ANOVA with subsequent Tukey's post hoc test or Mann-Whitney if data were not normally distributed. Significance was set at $p<0.05$.

RESULTS

Adipose *Phd2* Deficiency Stabilizes HIFα Levels and Up-regulates HIFα Target Genes. We studied inter-cross progeny of the littermate genotype *Phd2*$^{lox/lox}$ mice (control, designated *Phd2*; described in 35, 39) with the *Fabp-4-Cre* (aP2-Cre) mice (38) to make an adipose tissue selective *Phd2* deficiency model designated aP2-*Phd2*KO. Efficient recombination was detected in epididymal (epi), mesenteric (mes) and brown (BAT) adipose tissue and in isolated epididymal adipocytes (Supplemental Fig. 1*A*). Recombination was observed in the whole stromal vascular fraction (SVF), but there was no evidence for recombination in macrophages (Supplemental Fig. 1*A*). PHD2 mRNA (Fig. 1*A*) and protein was efficiently knocked down (~70%) in aP2-*Phd2*KO adipose tissue (Fig. 1*B*) and in primary adipocytes (Fig. 1*C)* cultured *in vitro.* No significant *Phd2* recombination was found in other tissues such us heart, muscle, spleen or liver (Supplemental Fig. 1*B*). Adipose *Phd1* and *Phd3* mRNA levels were unaffected (Supplemental Fig. 1*C*). Hypoxia markedly up-regulated *Phd2* mRNA levels *in vitro* (3-fold, $p<0.0001$) in control adipocytes, but this induction was absent in aP2-*Phd2*KO adipocytes (Fig. 1*D*).

Homozygous deletion of *Phd2* in adipocytes led to stabilization of HIF-1α and HIF-2α protein levels in adipose under normoxic conditions (Fig. 1E-F). HIF target genes encoding proteins for nutrient metabolism (*Glut1, Glut4, Pdk1, Pdk4*) and angiogenesis (*Vegfa, Angpl4, Tgfb*) were higher in white adipose tissue of aP2-*Phd2*KO compared to control littermates (Fig. 2*A*). Hypoxia led to significantly higher mRNA levels of *Glut1* and *Vegfa* in isolated aP2-*Phd2*KO than control adipocytes (Fig. 2*B*). In order to evaluate which *Hifa* isoform dominantly regulates target genes in the aP2-*Phd2*KO model, we measured mRNA levels of the same genes in mice with adipose-specific deletion (aP2-Cre-driven deletion) of *Hif1*a (aP2-*Hif1*aKO) or *Hif2a* (aP2-*Hif2a*KO), which blunts the hypoxia-induced stabilization of HIF1α in adipocytes (Supplemental Fig. 2*A*). Deletion of *Hif1a* in adipose

tissue reduced the mRNA levels of genes that control nutrient metabolism (*Glut1, Pdk1, Pdk4*) and the pro-fibrotic response (*Tgfb*), with pronounced effects in high fat fed animals (Fig. 2*C*). This effect was localised to mature adipocytes (Supplemental Fig. 2 *B*). In contrast, adipose *Hif2a* deletion reduced the mRNA levels of angiogenic genes (*Vegfa, Angpl4)* (Fig.2*D*) indicating a predominant role for HIF2a in adipose vascularization.

Adipose *Phd2* Deficiency Increases Adiposity in Parallel with Increased Adipose Vascularization.

Chow diet (low fat)-fed aP2-*Phd2*KO mice exhibited increased adiposity by 19 weeks of age compared to control littermates (Fig. 3*A*), with ~2-fold higher cumulative weight gain from 9-30 weeks (Fig. 3*B*). Adult aP2-*Phd2*KO mice had more white adipose tissue mass (>50%) in all depots, but brown adipose and liver masses were unaltered (Fig. 3*C*). Body and adipose tissue weight differences were not due to increased food intake (Fig. 3*D*). As expected for their higher adiposity, aP2-*Phd2*KO mice showed a parallel increase in plasma leptin levels (Table 1).

Adipose *Phd2* Deficiency Maintains Glucose Tolerance Associated with Suppressed Lipolysis and Reduced Ectopic Lipid Accumulation.

Despite increased adiposity, aP2-*Phd2*KO mice exhibited normal glucose tolerance (Fig. 3*E*) and similar fasted and fed plasma insulin levels (Table 1) to their control littermates. aP2-*Phd2*KO mice had comparable ad libitum-fed but reduced fasting NEFA levels (after 5 hour or overnight fast, Table 1 & Fig. 3*F*). Notably, aP2-*Phd2*KO mice exhibited blunted β-adrenergic agonist CL316,243 responsiveness *in vivo* (Fig. 3*F*), with significantly reduced NEFA release. Liver and muscle triglyceride (TAG) levels were lower in aP2-*Phd2*KO mice (Fig. 3*G*).

Greater fat deposition in aP2-*Phd2*KO mice was associated with larger adipocytes (diameter 230±12μm, 177±18μm in controls, p=0.034) (Fig. 4*A*). However, adipose *Phd2* deficiency did not affect adipose macrophage density (Fig. 4*B*) or fibrosis (Fig. 4*C*, Supplemental Fig. 3), markers of inflamed and hypoxic adipose tissue respectively. Intriguingly, adipose *Phd2* deficient mice manifested ~2-fold (p=0.001) greater density of immuno-staining for the endothelial marker CD31 in adipose tissue indicating an enhanced vascular expansion (Fig. 4 *D-E*).

Because *Phd2* deficiency in the model presented here stabilizes both HIFα isoforms, we attempted to dissect the role of different HIFα isoforms in adipocyte function *in vivo*. Therefore, aP2-*Hif1*aKO or aP2-*Hif2*aKO deficient mice were analysed. Chow-fed aP2-*Hif1*aKO or aP2-*Hif2*aKO were comparable to control littermates (data not shown), therefore these mice were analysed after 12 weeks exposure to high fat feeding. Notably, *Hif1*a-deleted mice manifested reduced body weight gain and improved glucose tolerance on high fat diet (Supplemental Fig. 4*A*-*C*). In contrast, adipose tissue *Hif2*-deleted mice fed a high fat diet gained similar body weight (Supplemental Fig. 4*D*) but showed worsening of glucose tolerance (Supplemental Fig. 4*E*) and elevated fasting insulin (Supplemental Fig.4*F*), suggesting insulin resistance. There was no difference in plasma fasting NEFA or liver triglyceride levels in aP2-*Hif2*aKO or aP2-*Hif2*aKO mice compared to their littermate controls (Supplemental Table 1).

Adipose *Phd2* Deficiency Leads to Suppression of Lipolytic Signalling.

To investigate the mechanism by which adipose *Phd2* deficiency drives adipocyte hypertrophy we assessed lipolytic responses of the adipocytes *in vitro* under normoxic (21% O_2) and hypoxic (1% O_2) conditions. In normoxia, basal and β-adrenergic–stimulated NEFA release into the medium of aP2-*Phd2*KO adipocytes was significantly lower than control (Fig. 5*A*). The reduced lipolytic response of aP2-*Phd2*KO adipocytes was also apparent under

hypoxic conditions; hypoxia itself attenuated stimulated but not basal lipolysis (Fig. 5*A*). The reduced NEFA release from *Phd2*-deficient adipocytes was associated with reduced levels of the key lipolytic proteins, hormone sensitive lipase (HSL) and perilipin (Fig. 5*B- C,* 5*E*). Lower HSL mRNA was also observed in aP2-*Phd2*KO adipose tissue, whereas perilipin mRNA levels were unaltered (Fig. 5*G*). In contrast, the mRNA of the triglyceride synthesis gene diacyglycerol acylotransferase-1 (*Dgat1*) was higher in aP2-*Phd2*KO adipose tissue. Supporting the HIF1α-dependence of this effect, adipocytes from aP2-*Hif1*aKO and not aP2-*Hif2*aKO mice showed a higher basal and β-adrenergic-stimulated NEFA release in hypoxia (Fig. 5*H*) as well as higher total HSL and perilipin protein levels (Fig. 5*I-J* and quantification in Supplemental Fig. 5*A-C*). Consistent with this, *Hif2*a-deficient adipocytes showed normal NEFA release and HSL levels (Supplemental Fig. 6*A-C*). Short-term activation of HSL is mediated by phosphorylation at Serine 660 (PKA-mediated) and Serine 565 (AMPK-mediated) (42). Immunoblotting revealed that PHD/HIF-1α affected total HSL protein levels but not the phosho-HSL/total HSL protein ratio (Fig. 5 *D* and *F* and Supplemental Fig. 5 *C*). In addition, *Phd2 deficiency* increased expression of the main anti-lipolytic alpha-2 adrenergic receptor and tended to decrease levels of the lipolytic β3 adrenergic receptor, consistent with greater anti-lipolytic tone in aP2-*Phd2*KO adipose tissue (Fig. 5*G*).

Pharmacological Inhibition of HIF-Prolyl Hydroxylases Suppresses Murine and Human Adipocyte Lipolysis.

We next explored the effect on lipolysis of a small molecule PHD inhibitor (PHI) that activates HIFα robustly (40-41). Pharmacological inhibition of PHDs in mouse adipocytes by PHI led to a significant stabilization of HIF1α protein levels (10-fold, p=0.026) and to a lesser extent HIF2α (Fig. 6*A*). In both murine (Fig. 6*B*) and human (Fig. 6*C*) primary adipocytes, PHI elicited a profound suppression of basal and adrenergic agonist-stimulated NEFA release in normoxia. As was observed in *Phd2*-deficient adipocytes (aP2-*Phd2*KO),

total ATGL was not affected but HSL and perilipin protein levels were lower in the PHI-treated adipocytes (Fig. 6*D-E*) with no effect on the ratio of phosphorylated HSL to total HSL (Fig. 6*D*) after adrenergic stimulation. PHI-treatment reduced basal ATGL levels (Fig. 6*F*).

Administration of PHI to mice *in vivo* supressed basal plasma NEFA and β-adrenergic-stimulated NEFA release (Fig. 6*G*). This effect was consistent with a selective down-regulation of HSL mRNA levels in adipose tissues from PHI-treated C57BL/6 mice (Fig 6*H*). In human adipocytes *in vitro*, isoproterenol increased the phosphorylation of AKT (Ser-473) in both vehicle and PHI-treated adipocytes (Fig. 6*I*). However, the ratio of phospho-AKT (Ser-473) to total AKT was higher in the PHI-treated human adipocytes (Fig. 6*I*) suggesting selective enhancement of insulin sensitivity with PHD inhibition.

Adipose *PHD2* mRNA Levels Correlate with mRNA Levels of Lipolytic Genes in a Depot-specific Manner in Humans.

We further extended our findings on the role of PHD2 in adipose tissue in a cohort of type 2 diabetics. Adipose *PHD2* (*EGLN1*) mRNA levels did not correlate with crude measures of obesity (BMI; Table 2). However, *PHD2* mRNA levels positively correlated with mRNA for caveolin (*CAV1*), a co activator of the lipolytic protein *ATGL*, *ABHD5* and another lipolytic cascade-modulating gene, the a-kinase anchoring protein (*AKAP*). Notably, Type 2 diabetics had lower subcutaneous adipose tissue (SAT) *PHD2* mRNA levels than non-diabetics (Table 2).

DISCUSSION

Here we describe a novel biological role for "pseudohypoxia" (see Fig. 7) in the suppression of adipocyte lipolysis. Genetic *Phd2* deficiency resulted in an increased adipose mass, but with normal glucose tolerance and reduced circulating levels of fatty acids. This apparently protective adipose expansion was associated with increased vascularity and no increase in adipose tissue macrophage burden or fibrosis. Mechanistic dissection revealed that in isolated mouse adipocytes *in vitro*, basal and β-adrenergic-stimulated release of NEFA was reduced by genetic inactivation of *Phd2*. Importantly, these findings were recapitulated by the acute exposure of mouse and human adipocytes to a selective prolyl hydroxylase inhibitor that targets PHD2.

In oxygenated cells, the HIF prolyl hydroxylases promote degradation of HIFα sub-units following association of hydroxylated HIF with the VHL ubiquitin E3 ligase. PHD2 is the most abundant of these enzymes and is the most important in setting levels of HIF activity in normoxic cells (20). Thus, PHD2 inactivation by genetic or pharmacological means is predicted to mimic hypoxia, creating a "pseudohypoxic" signal that activates the HIF transcriptional cascade in normoxic conditions. Although we cannot be certain that all the effects we observed were mediated by this mechanism, several lines of evidence support this. First, both HIFα proteins and HIF transcriptional target genes were induced in adipose tissues and cells by these interventions. Second, genetic inactivation of *Hif1a* revealed effects that were consistent with induction of HIF being responsible for at least some of the observed effects of *Phd2* inactivation. In particular, inactivation of *Hif1a* in adipose tissues resulted in reduced body weight gain with high fat feeding, and enhanced lipolytic responses in adipocytes. We therefore propose a model in which *Phd2* inactivation leads to co-ordinated activation of HIF pathways including marked up-regulation of *Vegfα* and *Angptl4* (most likely through HIF2a activation) with concomitant suppression of the key lipolytic enzyme

HSL and up-regulation of lipogenesis through *Dgat1* to increase fat cell lipid storage. We extended our findings to show a positive correlation between *PHD2* and *ABHD5* in SAT in humans. We also found a negative correlation between *PHD2* mRNA with mRNA for the lipid droplet protein-encoding genes perilipin or TIP47. These data support a role for oxygen sensing as an endogenous regulator of adipose tissue lipid mobilisation in humans and suggests PHD2 inhibition could promote metabolically protective peripheral fat accumulation. In this regard, reduced adipose perilipin protein levels in the ap2-*Phd2*KO mouse model was an unexpected finding, as this might be predicted to promote lipolysis. The regulation of the lipolytic machinery is complex and future work will investigate perilipin phosphorylation and indeed other lipid droplet protein levels that may reconcile the clearly anti-lipolytic effects of PHD inhibition at this functional level.

A number of observational studies have implicated adipose hypoxia in the pathogenesis of insulin resistant-obesity (2-4). Furthermore, several groups have generated transgenic mouse models of HIF1α modulation in adipose tissue. Some (5, 29-32), but not all (28, 43, 44) of these studies have reported that elevated levels of HIF1α lead to obesity, with fibrotic scarring and insulin resistance in the adipose tissue. Consistent with this, genetic inactivation or pharmacological inhibition of the HIF system is protective against obesity and its associated metabolic abnormalities (32, 33). Surprisingly, overexpression of HIF1α specifically in adipose tissue did not induce canonical HIF-target genes (*Vegfa* and *Glut1*) or affect the local adipose tissue angiogenic phenotype (5). Instead, HIF1α overexpression caused a pro-fibrotic adipose gene expression profile with associated histological abnormalities (5). These contrasting findings may reflect context-dependent regulation of overlapping target genes by the pleiotropic HIFs. Underlining this complexity, a recent study showed no obvious phenotypic changes under normal dietary conditions with an adipose-selective *Phd2* deletion mouse model analogous to ours (43). Indeed, this study reported

obesity-resistance in adipose *Phd2*-deleted mice (43) in contrast to previous reports showing HIF1α activation leads to an obese phenotype (5, 29-32). Moreover, obesity-resistance in the adipose-selective *Phd2*-deleted mice became apparent only after chronic high fat feeding (43) The reasons for the discrepancy between these studies could reflect differences in mouse strain genetic background, age, dietary intervention and the level of *Phd2* deletion achieved. Moreover, we did not observe a compensatory Phd3 up-regulation in our ap2-*Phd2*KO model, in contrast to Matsuura *et al* (43). Finally, while this manuscript was in revision, another study using a hypomorphic *Phd2* mutant mouse model of whole-animal PHD2 deficiency showed an improved metabolic profile with reduced adiposity (44). Complementary findings between our study and that of Rahtu-Korpela *et al*., are promising in terms of the therapeutic potential of PHD inhibitors to improve cholesterol (44) as well as reduced plasma NEFA levels (our study) and differences in adiposity phenotypes likely reflect our distinct tissue-specific effects versus those of whole-animal *Phd2* hypomorphicity. In any case, the focus of the work presented here is the effect of PHD/HIF signalling on adipocytes in mice and humans under normal dietary conditions and not under obesogenic conditions. Indeed, we have shown high fat diets regulate the PHD system (7) thus may potentially confound important baseline differences.

Of note, enlarged adipocytes but normal GTT responses were reported in a distinct genetic mouse model of adipose-specific HIF-α activation caused by ablation of the Von Hippel–Lindau tumour suppressor (VHL; a factor degrading HIF downstream of PHD action) (45). The adipose-specific VHL knockout model exhibited a cardiac hypertrophy phenotype resulting from severe adipose inflammation and highlighted the effect of manipulating distinct HIF-α isoform levels (45). We show that targeting PHDs, as opposed to VHL, also reveals distinct effects and our findings are key in order to fully evaluate which components of the HIF signalling pathway are relevant to metabolic pathologies.

The “pseudohypoxic” induction of HIF caused by *Phd2* deletion may effectively “pre-empt” the remodelling effects normally caused by local hypoxia when fat rapidly expands in obesity. This may prime adipose tissue to resist the inflammatory and fibrotic responses seen with vascular rarefaction in obesity, by activating the pro-angiogenic factors such as *Angptl4* and *Vegfa* and coordinating more effective vascular remodelling to cope with fat deposition (5, 30, 32). Inactivation of *Phd2* better mimics the co-ordinated physiological activation of all isoforms of HIF system than over-expression of a single isoform. Thus, although in many cells PHD2 has greater activity on HIF1α than HIF2α (46), we observed that inactivation of *Phd2* deficiency in adipose tissue is also associated with stabilization of HIF2α. A large body of data now indicates that HIF1α and HIF2α have different, and sometimes opposing, biological effects (47). In keeping with this, we observed entirely different responses to the inactivation of HIF1α and HIF2α in adipose tissues. Although inactivation of HIF2α did not result in altered adipose mass under the experimental conditions used, this does not preclude concurrent activation of HIF2α contributing to the phenotype associated with *Phd2* deficiency. Indeed, HIF2α is most likely involved in the pro-angiogenic response of aP2-*Phd2*KO mice. It is also possible that quantitative differences in the extent of HIF pathway activation underlie the differences in adipose phenotypes, as has been observed in the heart (45, 48) and pancreatic β-cell (49, 50) where pronounced induction of HIF is associated with organ dysfunction, but modest induction has beneficial effects on metabolic function or protection from ischemia.

Our work reveals a novel role for the oxygen sensor PHD2 in the regulation of adipocyte lipolysis. PHD2 inhibition suppresses lipolysis and promotes angiogenic responses through distinct HIF isoform activation thereby promoting benign adipose tissue expansion. Notably, PHD inhibitors similar to those used in this study are under clinical trials for anemia and ischemia (33-34). Although the effects of PHD inhibition in metabolic disease remain to be

tested, our data suggest that selective PHD2 inhibition may also be beneficial for ameliorating the detrimental metabolic consequences of elevated fatty acid levels found in insulin-resistant obesity and lipodystrophic dyslipidaemia.

ACKNOWLEDGEMENTS

This work was funded by a Henry Wellcome Postdoctoral Fellowship (ZM; 085458/Z/08/Z) and a British Heart Foundation/University of Edinburgh Centre of Research Excellence Transition Award Fellowship (ZM). We thank Tammie Bishop and Ya-Min Tian (Ratcliffe Laboratory, Oxford) for advice on the use of PHD inhibitors, Xantong Zou, Rhona Aird and Karen French for excellent technical assistance and the staff in the BRR facility (Edinburgh) for maintenance of the mouse colony. We wish to thank Professors Nicholas Hastie, Stewart Forbes and John Iredale (Edinburgh) for useful discussions.

ZM designed, performed experiments, analysed data and wrote the manuscript. NMM designed, performed experiments, contributed to discussion and reviewed/edited manuscript. CCW and KJS provided the human adipose biopsies. JMMN and JMFR designed, performed and analysed the human diabetic cohort gene expression study. CJS provided essential reagents and reviewed /edited the manuscript. JRS contributed to discussion and reviewed/edited manuscript and PJR provided the *Phd2* homofloxed mice, contributed to discussion and reviewed/edited manuscript.

ZM is the guarantor of this work and, as such, had full access to all of the data in the study and takes responsibility for the integrity of the data and the accuracy of the data analysis.

Conflict of interest statement: PJR and CJS are scientific co-founders and hold equity in ReOx Ltd, a company which is seeking to develop HIF hydroxylase inhibitors for therapeutic use.ZM, NMM, CCW, KJS, JMMN, JMFR and JRS have no conflict of interest to declare.

REFERENCES

1. Pasarica M, Sereda OR, Redman LM, Albarado DC, Hymel DT et al. Reduced adipose tissue oxygenation in human obesity: evidence of rarefaction, macrophage chemotaxis and inflammation without an angiogenic response. *Diabetes* 2009; 58:718-725

2. Gealekman O, Guseva N, Hartigan C, Apotheker S, Gorgoglione M et al. Depot-specific differences and insufficient subcutaneous adipose tissue angiogenesis in human obesity. *Circulation* 2011;123: 186-194

3. Trayhurn P, Wood IS. Adipokines: inflammation and the pleiotropic role of white adipose tissue. *Br J Nutr* 2004; 92:347-355

4. Hosogai N, Fukuhara A, Oshima K, Miyata Y, Tanaka S, et al. Adipose tissue hypoxia in obesity and its impact on adipocytokine dysregulation. *Diabetes 2007;*56: 901-911

5. Rausch M E, Weisberg S, Vardhana P, Tortoriello D V. Obesity in C57BL/6J mice is characterized by adipose tissue hypoxia and cytotoxic T-cell infiltration. *Int J Obes (Lon)* 2008;32: 451-463

6. Halberg N, Khan T, Trujillo ME, Wernstedt-Asterholm I, Attie AD et al. Hypoxia-inducible factor 1alpha induces fibrosis and insulin resistance in white adipose tissue. *Mol Cell Biol* 2009; 29: 4467-4483

7. Michailidou Z, Turban S, Miller E, Zou X, Schrader J et al. Increased angiogenesis protects against adipose hypoxia and fibrosis in metabolic disease-resistant 11β-hydroxysteroid dehydrogenase type 1 (HSD1)-deficient mice. *J Biol Chem* 2012;287:4188-4197

8. Sun K, Wernstedt Asterholm I, Kusminski CM, Bueno AC, Wang ZV et al. Dichotomous effects of VEGF-A on adipose tissue dysfunction. *Proc Natl Acad Sci U S A* 2012;109:5874-5879

9. Elias I, Franckhauser S, Ferré T, Vilà L, Tafuro S et al. Adipose tissue overexpression of vascular endothelial growth factor protects against diet-induced obesity and insulin resistance. *Diabetes* 2012;61:1801–1813

10. Sung HK, Doh KO, Son JE, Park JG, Bae Y et al. Adipose vascular endothelial growth factor regulates metabolic homeostasis through angiogenesis. *Cell Metab* 2013;17:61-72

11. Virtue S, Vidal-Puig A. Adipose tissue expandability, lipotoxicity and the Metabolic Syndrome--an allostatic perspective. *Biochim Biophys Acta* 2010; 1801:338-349

12. Ebbert JO and Jensen MD. Fat depots, Free Fatty Acids and Dyslipidemia. *Nutrients* 2013;5:498-508

13. Sun K, Kusminski CM, Scherer PE. Adipose Tissue Remodeling and Obesity. *J Clin Invest* 2011;121:2094-101

14. Rupnick MA, Panigrahy D, Zhang CY, Dallabrida SM, Lowell BB et al. Adipose tissue mass can be regulated through the vasculature. *Proc Natl Acad Sci U S A*. 2002;99:10730-10735

15. Hausman GJ, Richardson RL. Adipose tissue angiogenesis. *J Anim Sci*2004;82:925-934

16. Cao Y. Angiogenesis modulates adipogenesis and obesity. *J Clin Invest* 2007; 117:2362-2368

17. Semenza GL. Oxygen Homeostasis. *Wiley Interdiscip Rev Syst Biol Med*. 2010; 2:336-361

18. Yun Z, Maecker HL, Johnson RS, Giaccia AJ.Inhibition of PPAR gamma 2 gene expression by the HIF-1-regulated gene DEC1/Stra13: a mechanism for regulation of adipogenesis by hypoxia. *Dev Cell* 2002;2:331-341

19. Shimba S, Wada T, Hara S, Tezuka M. EPAS1 promotes adipose differentiation in 3T3-L1 cells. *J Biol Chem 2004;* 279:40946-40953

20. Ratcliffe PJ. Oxygen sensing and hypoxia signalling pathways in animals: the implications of physiology for cancer. *J Physiol 2013;* 591:2027-2042

21. Bruick RK, McKnight SL. A conserved family of prolyl-4-hydroxylases that modify HIF. *Science* 2001; 294:1337-1340

22. Epstein AC, Gleadle JM, McNeill LA, Hewitson KS, O'Rourke J et al. C elegans EGLN-9 and mammalian homologs define a family of dioxygenases that regulate HIF by prolyl hydroxylation. *Cell* 2001; 107:43-54

23. Ivan M, Kondo K, Yang H, Kim W, Valiando J et al. HIFalpha targeted for VHL-mediated destruction by proline hydroxylation: implications for O2 sensing. *Science* 2001; 292:464-468

24. Jaakkola P, , Mole DR, Tian YM, Wilson MI, Gielbert J et al. Targeting of HIF-alpha to the von Hippel-Lindau ubiquitylation complex by O2-regulated prolyl hydroxylation. *Science* 2001; 292 :468-472

25. Floyd ZE, Kilroy G, Wu X, Gimble JM. Effects of prolyl hydroxylase inhibitors on adipogenesis and hypoxia inducible factor 1 alpha levels under normoxic conditions. *J Cell Biochem* 2007; 101:1545-1457

26. Regazzetti C, Peraldi P, Grémeaux T, Najem-Lendom R, Ben-Sahra I et al. Hypoxia decreases insulin signaling pathways in adipocytes. *Diabetes* 2009; 58:95-103

27. Zhang X, Lam KS, Ye H, Chung SK, Zhou M et al. Adipose tissue specific inhibition of hypoxia-inducible factor 1α induces obesity and glucose intolerance by impeding energy expenditure in mice. *J Biol Chem* 2010; 285:32869-32877

28. He Q, Gao Z, Yin J, Zhang J, Yun Z, Ye J. Regulation of HIF-1alpha:Activity in adipose tissue by obesity-associated factors: Adipogenesis, Insulin and Hypoxia. *Am J Physiol Endocrinol Metab* 2011; 300:E877-E885

29. Jiang C, Qu A, Matsubara T, Chanturiya T, Jou W et al. Disruption of hypoxia-inducible factor 1 in adipocytes improves insulin sensitivity and decreases adiposity in high-fat diet-fed mice. *Diabetes* 2011; 60:2484-2495

30. Lee KY, Gesta S, Boucher J, Wang XL, Kahn CR. The differential role of Hif1β/Arnt and the hypoxic response in adipose function, fibrosis, and inflammation. *Cell Metab* 2011;14:491-503

31. Krishnan J, Danzer C, Simka T, Ukropec J, Walter KM et al. Dietary obesity-associated Hif1α activation in adipocytes restricts fatty acid oxidation and energy expenditure via suppression of the Sirt2-NAD+ system. *Genes Dev* 2012;26:259-270

32. Sun K, Halberg N, Khan M, Magalang UJ, Scherer PE.Selective inhibition of hypoxia-inducible factor 1α ameliorates adipose tissue dysfunction. *Mol Cell Biol* 2013; 33:904-917

33. Hewitson KS, McNeill LA, Schofield CJ. Modulating the hypoxia-inducible factor signaling pathway: applications from cardiovascular disease to cancer. *Curr Pharm Des* 2004; 10:821-833

34. Fraisl P, Aragonés J, Carmeliet P. Inhibition of oxygen sensors as a therapeutic strategy for ischaemic and inflammatory disease. *Nat Rev Drug Discov* 2009;8:139-152

35. Mazzone M, Dettori D, Leite de Oliveira R, Loges S, Schmidt T et al.Heterozygous deficiency of PHD2 restores tumor oxygenation and inhibits metastasis via endothelial normalization. *Cell* 2009; 136:839-850

36. Ryan HE, Poloni M, McNulty W, Elson D, Gassmann M et al. Hypoxia-inducible factor-1alpha is a positive factor in solid tumor growth. *Cancer Res* 2000; 60:4010-4015

37. Gruber M, Hu CJ, Johnson RS, Brown EJ, Keith B, Simon MC. Acute postnatal ablation of Hif-2alpha results in anemia. *Proc Natl Acad Sci U S A* 2007;104:2301-2306

38. He W, Barak Y, Hevener A, Olson P, Liao D et al. Adipose-specific peroxisome proliferator-activated receptor gamma knockout causes insulin resistance in fat and liver but not in muscle. *Proc Natl Acad Sci U S A* 2003;100: 15712–15717

39. Adam J, Hatipoglu E, O'Flaherty L, Ternette N, Sahgal N et al. Renal cyst formation in Fh1-deficient mice is independent of the Hif/Phd pathway: roles for fumarate in KEAP1 succination and Nrf2 signaling. *Cancer Cell* 2011; 20:524-537

40. Tian YM, Yeoh KK, Lee MK, Eriksson T, Kessler BM et al. Differential sensitivity of hypoxia inducible factor hydroxylation sites to hypoxia and hydroxylase inhibitors. *J Biol Chem* 2011; 286:13041-13051

41. Bishop T, Talbot NP, Turner PJ, Nicholls LG, Pascual A et al. Carotid body hyperplasia and enhanced ventilatory responses to hypoxia in mice with heterozygous deficiency of PHD2. *J Physiol* 2013;591:3565-3577

42. Girousse A, Langin D. Lipases and lipid droplet-associated proteins: insight from transgenic mouse models. *Int J Obes (Lond)* 2012; 36(4): 581-594.

43. Matsuura H, Ichiki T, Inoue E, Nomura M, Miyazaki R et al. Prolyl Hydroxylase Domain Protein 2 Plays a Critical Role in Diet-Induced Obesity and Glucose Intolerance. *Circulation* 2013;127:2078-2087

44. Rahtu-Korpela L, Karsikas S, Hörkkö S, Sequeiros RB, Lammentausta E et al. HIF prolyl 4-hydroxylase-2 inhibition improves glucose and lipid metabolism and protects against obesity and metabolic dysfunction. *Diabetes* 2014 [Epub ahead of print]

45**.** Lin Q, Huang Y, Booth CJ, Haase VH, Johnson RS et al. Activation of Hypoxia-Inducible Factor 2 in Adipocytes Results in Pathological Cardiac Hypertrophy. J Am Heart Assoc 2013;2;e000548

46. Huang J, Zhao Q, Mooney SM, Lee FS. Sequence determinants in hypoxia-inducible factor-1alpha for hydroxylation by the prolyl hydroxylases PHD1, PHD2, and PHD3. *J Biol Chem* 2002;277:39792-39800

47. Keith B, Johnson RS, Simon MC. HIF1a and HIF2a: sibling rivalry in hypoxic tumor growth and progression. *Nat Rev Cancer* 2012;12:9-22

48. Kerkelä R, Karsikas S, Szabo Z, Serpi R, Magga J et al. Activation of Hypoxia Response in Endothelial cells Contributes to Ischemic Cardioprotection. *Mol Cell Biol* 2013;33:3321-3329

49. Cantley J Selman C, Shukla D, Abramov AY, Forstreuter F et al.Deletion of the von Hippel-Lindau gene in pancreatic beta cells impairs glucose homeostasis in mice. *J Clin Invest 2009;*119:125-35

50. Cheng K, Ho K, Stokes R, Scott C, Lau SM et al. Hypoxia-inducible factor-1alpha regulates beta cell function in mouse and human islets. *J Clin Invest* 2010;120:2171-2183

Table 1. Plasma biochemistry in *Phd2* and aP2-*Phd2*KO mice.

	Phd2	**aP2-*Phd2*KO**	**p value**
Fed insulin(ng/ml)	3.7±0.8	3.8±0.7	0.87
Fasted (o/n) insulin(ng/ml)	0.08±0.02	0.1±0.01	0.21
Fasted (5h) insulin (ng/ml)	1.6±0.2	1.6±0.3	0.95
Fed leptin (ng/ml)	19.2±4.0	**37.2±3.7****	*0.009*
Fed NEFA (mmol/L)	0.8±0.06	0.6±0.09	0.23
Fasted (5h) NEFA(mmol/L)	1.1±0.09	**0.8±0.04***	*0.048*

Data are mean ±SEM (n= 6/group). Bold type and asterisks indicate significant differences between genotypes. NEFA, non-esterified fatty acids.

Table 2. PHD2 (EGLN1) correlations with genes involved in the lipolytic machinery in human subcutaneous (SAT) and visceral (VAT) adipose depots.

	Non-diabetic participants	**Type 2 diabetic participants**	**P value**
N	73	29	
Age (years)	47.23 ± 12.1	47.55 ± 11.3	0.9
BMI (kg/m2)	37.7 ± 11.3	41.6 ± 6.8	0.09
Fasting glucose (mg/dL)	93.01 ± 12.7	163.2 ± 59.8	**<0.0001**
EGLN1 (R.U.) in SAT	0.084 ± 0.021	0.070 ± 0.016	**0.002**
EGLN1 (R.U.) in VAT	0.082 ± 0.019	0.079 ± 0.020	0.4

	All participants		**Non-diabetic participants**		**Type 2 diabetic participants**	
SAT	r	p	r	p	r	p
Age (years)	-0.056	0.5	-0.047	0.7	0.046	0.8
BMI (kg/m2)	0.013	0.9	-0.001	0.9	-0.03	0.9
Fasting glucose (mg/dL)	-0.13	0.2	-0.015	0.9	0.17	0.3
CAV1 (R.U.)	0.47	**<0.0001**	0.46	**<0.0001**	0.46	**0.03**
ABHD5 (R.U.)	0.32	**0.01**	0.34	0.08	0.11	0.6
AKAP (R.U.)	0.32	**0.01**	0.36	0.06	0.55	**0.01**
ATGL (R.U.)	0.10	0.4	-0.10	0.5	0.12	0.6
MGLL (R.U.)	0.14	0.2	0.13	0.4	0.03	0.9
PRKACA (R.U.)	0.15	0.2	-0.11	0.4	0.68	**0.001**
PLIN1 (R.U.)	-0.15	0.2	-0.36	**0.04**	0.16	0.4
CIDEC (R.U.)	-0.01	0.9	-0.12	0.4	0.12	0.5
TIP47 (R.U.)	-0.27	**0.04**	-0.25	0.1	-0.14	0.5
VAT	r	p	r	p	r	p
Age (years)	-0.05	0.6	0.01	0.9	-0.17	0.3

BMI (kg/m2)	-0.08	0.4	-0.06	0.5	-0.16	0.3
Fasting glucose (mg/dL)	0.03	0.7	0.11	0.3	0.03	0.8
CAV1 (R.U.)	0.12	0.3	0.13	0.3	0.24	0.3
ABHD5 (R.U.)	0.07	0.6	-0.05	0.8	0.36	0.2
AKAP (R.U.)	0.07	0.5	0.01	0.9	0.21	0.4
ATGL (R.U.)	0.07	0.5	0.10	0.5	-0.01	0.9
MGLL (R.U.)	0.38	**0.004**	0.42	**0.008**	0.17	0.5
PRKACA (R.U.)	-0.06	0.6	-0.06	0.6	-0.12	0.6
PLIN1 (R.U.)	0.17	0.2	0.21	0.2	0.19	0.4
CIDEC (R.U.)	0.09	0.4	0.045	0.7	0.18	0.4
TIP47 (R.U.)	0.11	0.3	-0.02	0.9	0.38	0.1

FIGURE LEGENDS

FIG. 1.

Efficient aP2-Cre-Mediated Knock Down of PHD2 in Adipocytes stabilizes both HIFa isoforms. (*A*) Reduced *Phd2* mRNA levels in aP2-*Phd2*KO (black bars) white adipose tissue (WAT) compared to control *Phd2* littermates (white bars), n=5. **(*B*)** Representative western blot showing reduced PHD2 protein levels (upper panel, from left to right lanes 4-6) in aP2-*Phd2*KO WAT compared to control littermates (upper panel, lanes 1-3). Mouse embryonic fibroblasts lysates from *Phd2* wild type (+/+; lane 7) and *Phd2* knock out (-/-; lane 8) mice were included to identify specificity of the anti-PHD2 antibody. **(*C*)** Reduced PHD2 protein levels in aP2-*Phd2*KO adipocytes, quantification graph of a representative western blot **(*D*)** Reduced *Phd2* mRNA levels in isolated aP2-*Phd2*KO adipocytes cultured in normoxia (21%O_2) and ablated response to hypoxia (1%O_2). **(*E*)** Representative western blots and (F) quantification graph showing stabilization of both HIF1a and HIF2a in adipose tissue in aP2-*Phd2*KO adipose**.** mRNA was corrected to 18S and protein to beta ACTIN. Data are presented as arbitrary units (AU). * $p<0.05$, ** $p<0.01$, *** $p<0.001$ between genotypes. +++ $p<0.001$ comparison of hypoxia and normoxia within a genotype.

FIG. 2.

Adipose *Phd2* Deficiency Up-Regulates HIF-Target Genes in Normoxia.

(*A*) Up-regulation of HIF-a target genes in white adipose tissue of aP2-*Phd2*KO mice (black bars) compared to control *Phd2* littermates (white bars) n=7/group. ***(B)*** Isolated aP2-*Phd2*KO adipocytes showed higher mRNA levels of *Glut1* and *Vegfa* in both normoxia (21%O_2) and hypoxia (1%; 4hours), n=3/group. aP2-*Hif1a*KO (black bars, n=4-11/group) **(*C*)** and aP2-*Hif2a*KO (black bars, n-=4-6/group) ***(D)*** mice with their littermate controls (white bars) were fed a control diet or a high fat diet (HF, 58%kcal fat) for 12 weeks. mRNA levels of HIF-

target genes in adipose tissue was measured and corrected to 18S, data are presented as arbitrary units (AU). * p<0.05, ** p<0.01 and *** p<0. 001.

FIG. 3.

Adipose *Phd2* Deficient Mice Exhibit Increased Adiposity, Lower Plasma NEFA Levels and Reduced Triglyceride Levels in Liver and Muscle.

(*A*) Body weights in chow-fed aP2-*Phd2*KO (black squares-dashed line) are significantly higher after 18 weeks of age compared to Phd2 control mice (open circles-solid line) n=7/group. **(*B*)** aP2-*Phd2*KO mice (black bars) gain more weight between 9-30 weeks of age. **(*C*)** aP2-*Phd2*KO mice (black bars; n=7) have heavier white fat depots (SC; subcutaneous, EPI; epididymal and MES; mesenteric) but similar brown adipose tissue (BAT) and liver weights to control *Phd2* littermates (white bars; n=5). **(*D*)** Short term food intake was recorded between 14-16 weeks of age. There were no apparent differences in food intake between genotypes (n=5/group). (***E***) An intraperitoneal glucose tolerance test (2 mg/g BW glucose) in aP2-*Phd2*KO and control littermate mice (n=6/group). **(*F*)** Circulating non-esterified fatty acids (NEFA) concentrations in aP2-*Phd2*KO mice before and after stimulation with a lipolytic β-3 adrenergic agonist, CL316,243 (1μg/g BW i.p.) (n=5/group). ***(G)*** Liver and muscle triglyceride (TAG) levels in aP2-*Phd2*KO (black bars, n=6) and control littermate (white bars, n=8) mice. * p<0.05, ** p<0.01 between genotypes.

FIG. 4.

Adipose *Phd2* Deficiency Increases Adipocyte Size in Parallel with Increased Adipose Vasculature. (*A*) Bigger adipocytes in aP2-*Phd2*KO mice (black squares, n=6) compared to control littermates (open circles, n=5). **(*B*)** Similar macrophage numbers (F4/80 positive stained) in adipose tissue of aP2-*Phd2*KO mice. **(*C*)** Similar total collagen deposition

(Picrosirious Red staining) in aP2-*Phd2*KO adipose. **(*D*)** aP2-*Phd2*KO adipose tissue has more CD31 positive cells and vessels (arrows). **(*E*)** Quantification of total vessel number corrected for adipocyte number. Magnification x200. * $p<0.05$, ** $p<0.01$ between genotypes.

FIG. 5.

Phd2* Deficiency Suppresses Adipocyte Lipolysis *in vitro. **(*A*)** NEFA release in aP2-*Phd2*KO isolated adipocytes cultured in normoxia (21%O_2) or hypoxia (1%O_2) and stimulated with CL316,243 (100nM) for 4h show reduced lipolytic responses in both normoxia and hypoxia (n=4/group). Induction by CL treatment was significant but has been omitted for clarity. **(*B*)** Representative immunoblots of total ATGL, HSL and perilipin and phosphorylated HSL at serine 660 and 565 under basal and CL316,243 stimulation in normoxia. Labelling on blots WT; *Phd2* and KO; aP2*Phd2*KO. **(*C*)** Quantification (n=3/group) of immunoblots for total ATGL, HSL and perilipin levels corrected for beta ACTIN in normoxia. **(*D*)** Level of phosphorylated HSL corrected for total HSL in normoxia. Quantification of total HSL and perilipin proteins **(*E*)** and phosphorylated HSLs **(*F*)** in hypoxia. ***(G)*** mRNA levels of key genes involved in the regulation of the adipocyte lipolytic response, patatin-like phospholipase domain containing 2 (*Atgl*) , hormone sensitive lipase (*Hsl*), perilipin 1 (*Plin1*) and lipogenesis/ fatty acid uptake peroxisome proliferator-activated receptor gamma (*Pparg2*), fatty acid synthase (*Fasn*), stearoyl-CoA desaturase (*Scd1*), fatty acid translocase (*cd36*), diacylglycerol acylotransferases (*Dgat1* and *Dgat2*) and adrenergic signalling, β3-adrenergic receptor (*Adrb3*), α2-adrenergic receptor (*Adra2*) were measured in adipose tissue of aP2-*Phd2*KO mice (black bars, n=6/group) compared to control *Phd2* littermates (white bars, n=6/group). ***(H)*** NEFA release in the medium of aP2-*Hif1a*KO

adipocytes (black bars) cultured in normoxia (21%O_2) or hypoxia (1%O_2) and stimulated with CL316,243 show increased lipolytic response in hypoxia (n=4/group). Representative immunoblots of HSL and perilipin and phosphorylated HSL at serine 660 and 565 ***(I)*** Basal and ***(J)*** CL316,243 stimulated lipolysis during hypoxia. * $p<0.05$, ** $p<0.01$, ***$p<0.001$ comparisons between genotypes within treatment. $^{+}p<0.05$ indicates significant induction of p-HSL^{660} after CL316,243 stimulation in the control *Phd2*but not in the aP2-*Phd2*KO adipocytes.

FIG. 6.

Pharmacological Inhibition of HIF-Prolyl Hydroxylases Suppresses Murine and Human Adipocyte Lipolysis. Primary mouse (n=4/group) and human adipocytes (n=4/group) were pre-treated with a selective PHD inhibitor (PHI, 0.5mM) or vehicle (V;DMSO, 0.5%) for 1hour prior to a standard β-adrenergic stimulation of lipolysis by CL316,243 (100nM) or isoproterenol (100nM) for 3hours. Medium was collected for measuring NEFA concentrations and adipocytes were lysed for protein quantification and immunoblot analysis. **(*A*)** Representative blot shows significant stabilization of HIF1α levels and to a lesser extent HIF2α levels by PHI in mouse adipocytes (n=3/group) in normoxia. **(*B*)** Reduced basal and CL-stimulated NEFA release in PHI pre-treated mouse adipocytes. **(*C*)** Reduced basal and isoproterenol stimulated NEFA release in PHI pre-treated human adipocytes. **(*D*)** Representative mouse adipocyte immunoblots and ***(E)*** quantification graph shows unaltered ATGL but reduced HSL and perilipin levels after PHI treatment (n=3/group) in stimulated lipolysis. Note that ATGL is reduced by PHI in basal lipolysis ***(F)***. **(*G*)** *In vivo* administration of PHI i.p.(30mg/kg BW) 1h prior to CL i.p. (1μg/g BW) in C57BL/6 mice caused reduction of NEFA release compared to vehicle-treated (5% DMSO) mice and a reduced lipolytic response after CL316,243 administration (n=6/group). ***(H)*** mRNA levels of key lipolytic genes (corrected for 18S levels) in adipose tissue of C57BL/6 administered PHI i.p.

(30mg/kg BW, black bars) 1h prior CL316,243 i.p. (1μg/gr BW) or vehicle-treated (5% DMSO, white bars) mice administration (n=6/group). Immunoblots ***(I)*** and quantification graph ***(J)*** of phospho-AKT(Ser473), total AKT and ACTIN in human primary adipocytes pre-treated with PHI basally and after isoproterenol stimulation (n=3/group). * $p<0.05$, ** $p<0.01$, comparisons between PHI and V basally or after β-adrenergic stimulation. $^{+}p<0.05$ indicates that in human adipocytes only the vehicle group showed significant NEFA release after isoproterenol, the PHI group showed a blunted response.

FIG.7.

Schematic summary of the effects of pseudohypoxia in adipose tissue. During excessive fat accumulation in obesity (upper panel), the adipose tissue vasculature fails to facilitate this expansion and areas of hypoxia are created in adipose tissue (pink shaded areas). This leads to activation of HIF1a, recruitment of pro-inflammatory macrophages (light blue shapes), collagen deposition and fibrosis (thin brown lines), increased fatty acid release (lipolysis) , ectopic fat deposition and insulin resistance; pathological adipose expansion. In contrast, priming adipose tissue to be pseudo-hypoxic, by inhibiting the HIF-prolyl hydroxylases (genetic PHD2 deletion or pharmacological PHD inhibition), stabilises HIF1α and HIF2α. Adipose tissue expands due to reduced lipolysis and increased lipid storage, leading to reduced ectopic lipid deposition. This expansion does not alter the oxygen availability (green areas denote normoxia) in the tissue due to enhanced vascularization (red vessel shapes), thus leading to safe expansion without insulin resistance.

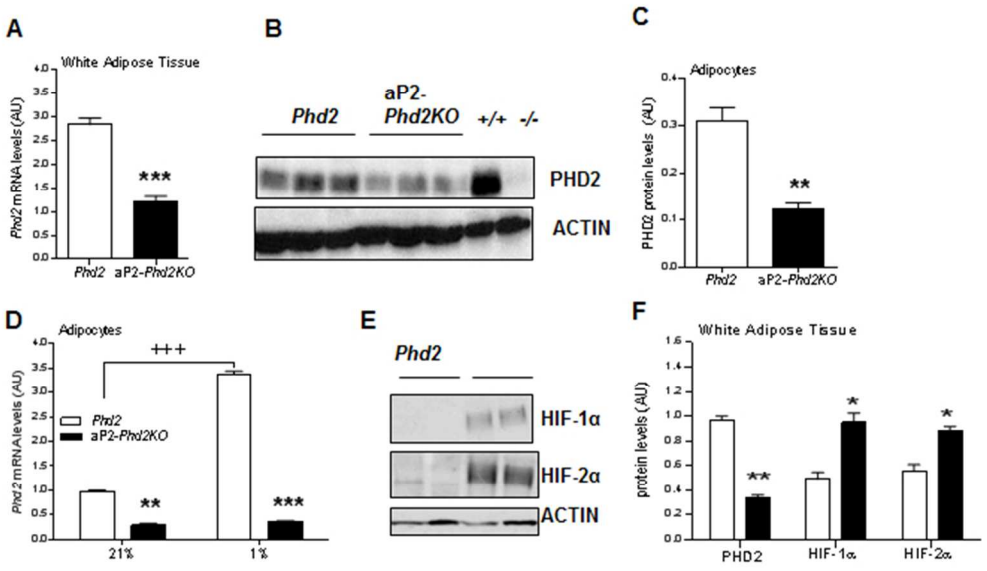

FIGURE 1
177x104mm (96 x 96 DPI)

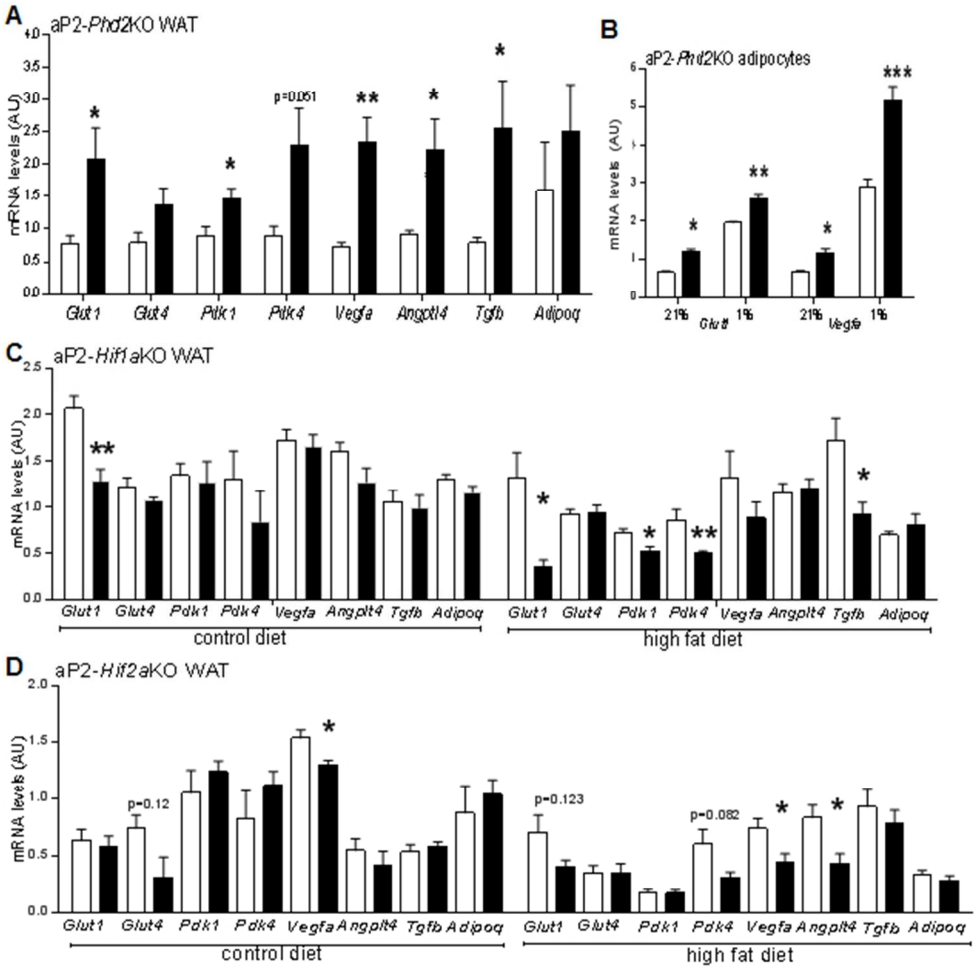

FIGURE 2
171x170mm (96 x 96 DPI)

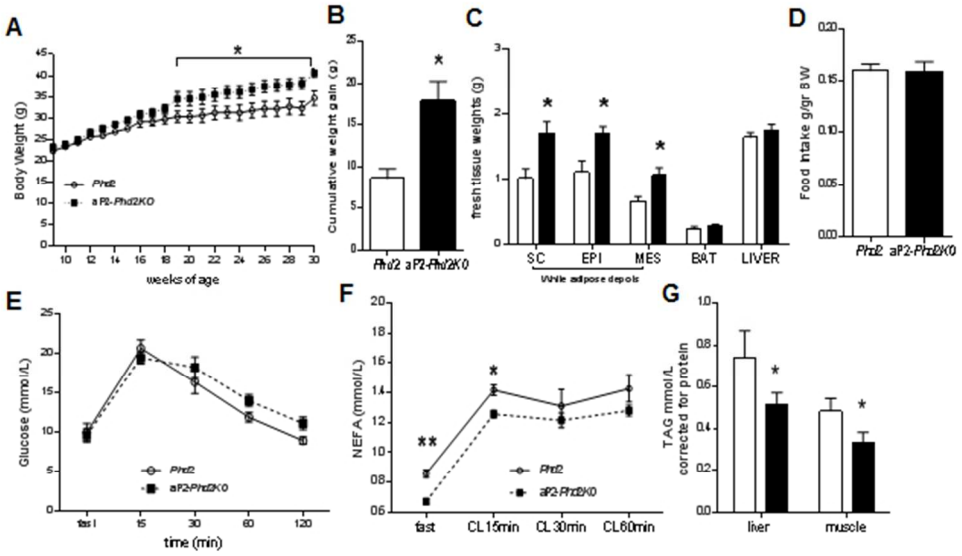

FIGURE 3
174x100mm (96 x 96 DPI)

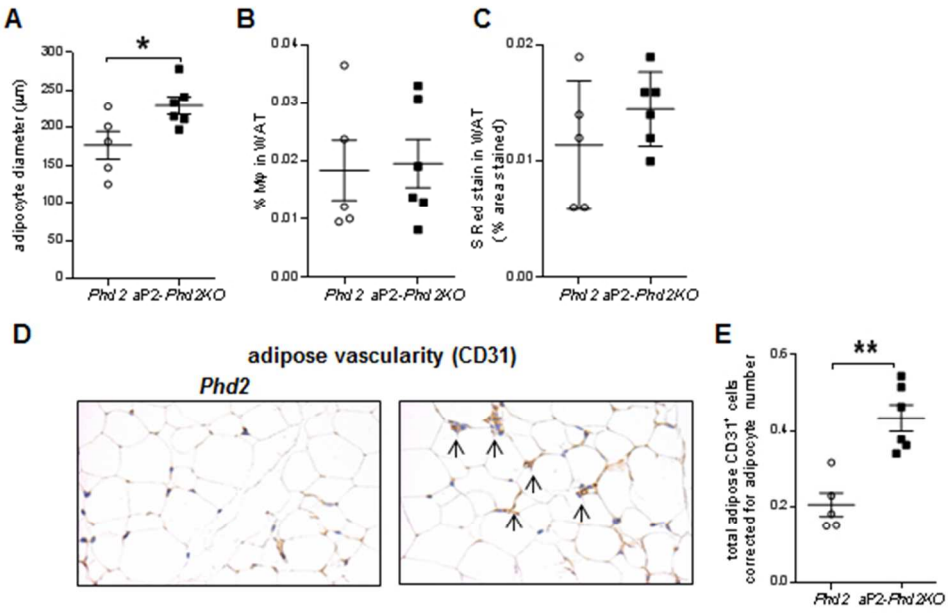

FIGURE 4
164x103mm (96 x 96 DPI)

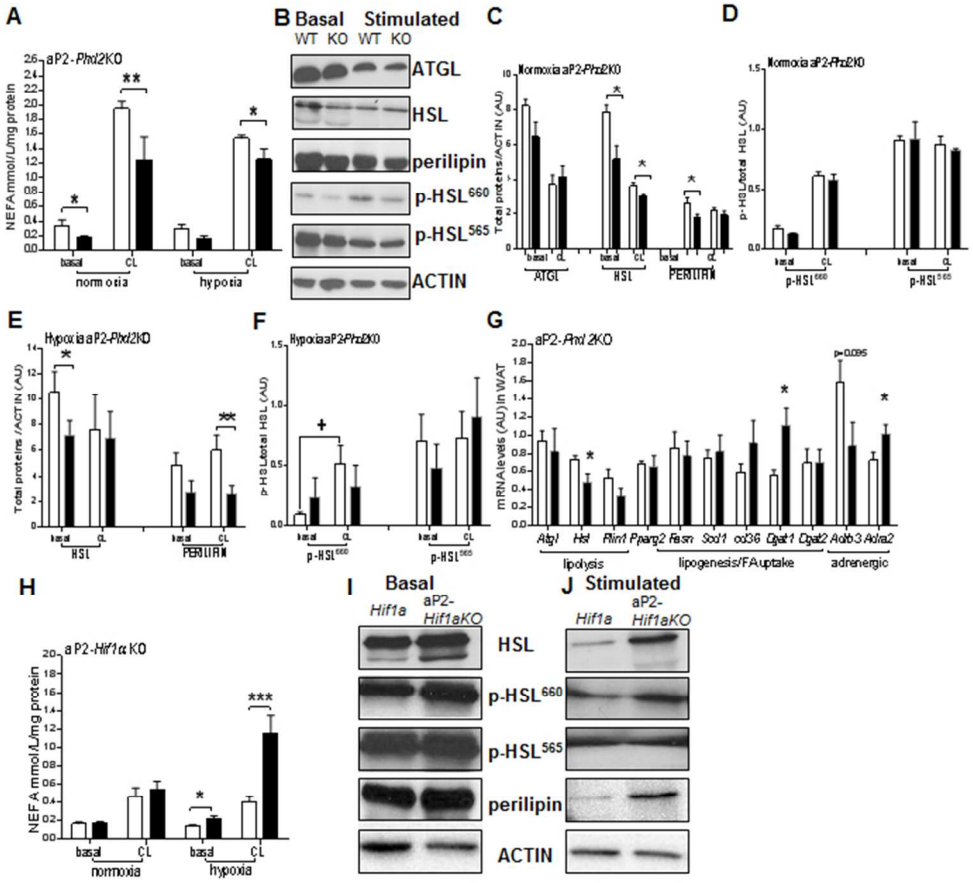

FIGURE 5 R2
188x169mm (96 x 96 DPI)

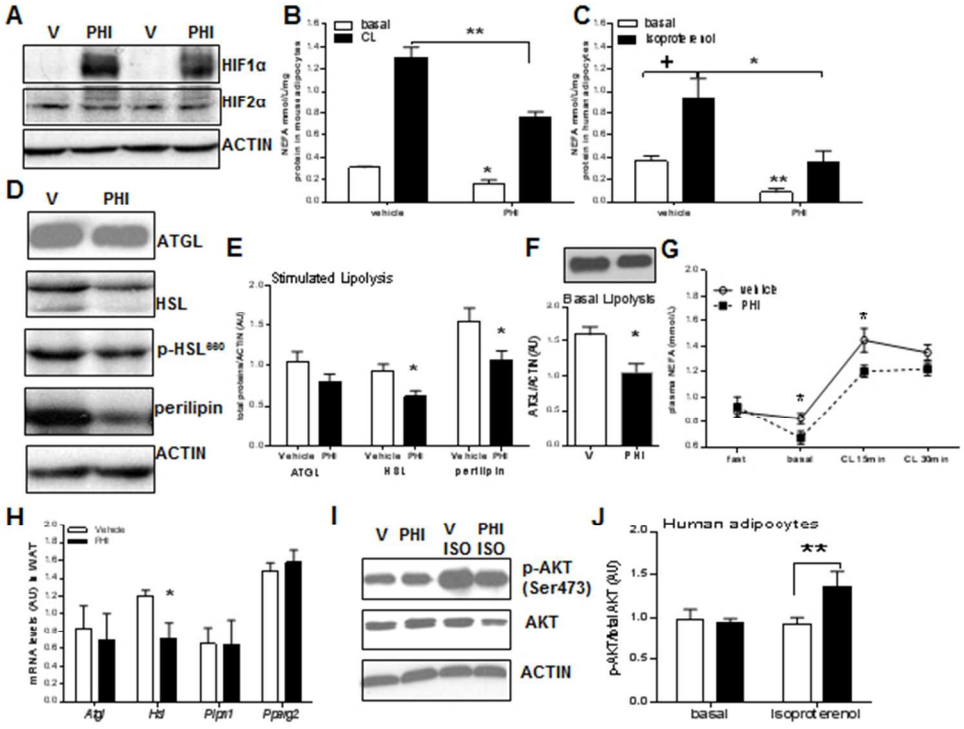

FIGURE 6 R2
171x128mm (96 x 96 DPI)

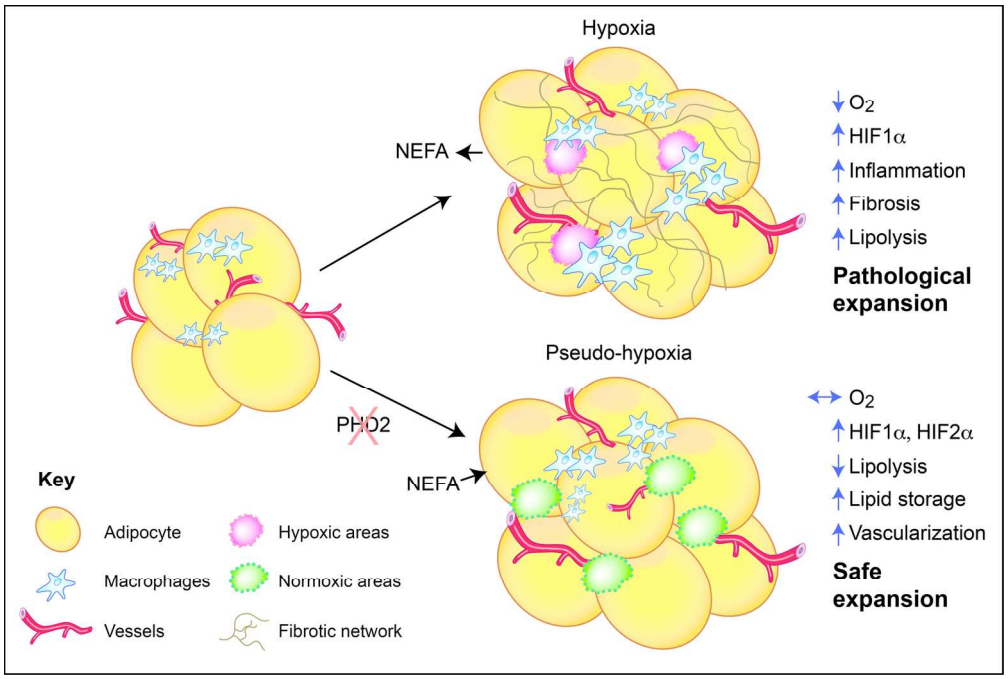

160x107mm (300 x 300 DPI)

Supplemental Table 1. Plasma NEFA and liver triglyceride levels in aP2-*Hif1a*KO and aP2-*Hif2a*KO mice under control and high fat diets.

	Hif1a **CD (n=6)**	**aP2-*Hif1a*KO CD (n=6)**	***Hif2a*** **CD (n=4)**	**aP2-*Hif2a*KO CD (n=4)**	***Hif1a*** **HFD (n=5)**	**aP2-*Hif1a*KO HFD (n=5)**	***Hif2a*** **HFD (n=4)**	**aP2-*Hif2a*KO HFD (n=4)**
Plasma NEFA mmol/L (5h fast)	1.0±0.07	0.9±0.08	0.8±0.02	1.0±0.05	1.1±0.1	1.1±0.04	0.8±0.05	0.8±0.03
Liver TAG mmol/L corrected for protein	0.4±0.07	0.3±0.07	0.2±0.03	0.2±0.05	1.3±0.05	1.2±0.07	1.1±0.16	1.2±0.15

Data are mean±SEM. CD, control chow diet. HFD, high fat diet (58% kcal fat). NEFA, non-esterified fatty acids and TAG, triglycerides.

Supplemental FIG. 1

Phd2* levels were not affected by adipocyte-specific *Phd2* deletion in other tissues.** ***(A) A schematic view (upper panel) of the genomic PCR used to detect the recombined *Phd2* allele (450bp)and agarose gel (lower panel) showing recombination in white adipose tissue depots (epi; epididymal, mes; mesenteric), brown adipose tissue (BAT) and isolated adipocytes (adipo). Note recombination in the stromovascular fraction (SVF) but not in isolated peritoneal macrophages (Mφ) in aP2-*Phd2*KO mice. ***(B)*** Recombination PCR gels show that there is no recombination (Cre-mediated excision) present in muscle, liver, spleen or heart in aP2-*Phd2*KO tissues. **(C)** Adipose *Phd2* deficiency (black bars) did not affect adipose *Phd1* or *Phd3* mRNA levels.

Supplemental FIG. 2

Hif1a* deficient adipocytes do not respond to hypoxic stimulus and have reduced HIFα target genes**. ***(A) Adipocytes from aP22-*Hif1a*KO mice (black bars, n=3) and *Hif1a* controls (white bars, n=3) were isolated and cultured in 21% O_2 or 1% O_2 for 6 hours. Cells were then lysed and probed with a HIF1α antibody. Representative blot (upper panel) and quantification graph (lower panel) showing significantly ablated HIF1α response in hypoxia in aP2-*Hif1a*KO adipocytes. ***(B)*** *Glut1* mRNA levels in isolated aP2-*Hif1a*KO adipocytes (black bars) are ~24 fold lower compared to control *Hif1a* adipocytes (white bars), n=3/group. mRNA levels are corrected for 18S and protein for beta ACTIN levels. AU; arbitrary units. * $p<0.05$, ** $p<0.01$, *** $p<0.001$ comparisons between genotypes. $^{+}p<0.05$ comparison of the effect of hypoxia within genotype.

Supplemental FIG. 3

Unaltered pro-fibrotic genes in adipose of aP2-*Phd2*KO mice. WAT mRNA levels of pro-fibrotic genes involved in adipose "scarring" such as collagens 1 (*Col1*), 3 (*Col3*), 6 (*Col6*),

matrix metalloproteinases 2 and 13 (*Mmp2, Mmp13*) and the collagen crosslinking protein lysyl oxydase (*Lox*) in **aP2-*Phd2*KO** mice (black bars, n=6) were similar to control littermate levels (white bars, n=5).

Supplemental FIG. 4

Opposing metabolic responses in aP2-*Hif1a*KO and aP2-*Hif2a*KO mice during High FatFeeding. aP2-*Hif1a*KO ***(A-C)*** and aP2-*Hif2a*KO ***(D-F)*** mice with their littermate controls were fed a High fat diet (HF, 58%kcal fat) for 12 weeks. ***(A)*** aP2-*Hif1a*KO (black squares-dashed line, n=6) gained less weight on a HF diet compared to control *Hif1a* mice (open circle-solid line, n=9). ***(B)*** aP2-*Hif1a*KO had similar glucose levels during oral glucose tolerance test (OGTT) at 6weeks (open square-dashed line) on HF diet to control mice and retained their glucose response after 12 weeks (black square-bold dashed line) on the diet, in contrast to control mice that showed impairment (open circle versus black circle, n=5/group). ***(C)*** Similar insulin levels during the OGTT (n=5/group). ***(D)*** aP2-*Hif2a*KO gained similar body weight to control *Hif2a* mice during HF. ***(E)*** aP2-*Hif2a*KO showed impaired response to OGTT at 6 and 12 weeks on HF diet and ***(F)*** aP2-*Hif2a*KO had higher basal fasting insulin during the OGTT compared to control littermates (n=6/group). * $p<0.05$, **$p<0.01$comparisons between genotypes and +$p<0.05$ comparisons of time (6-12 weeks) within genotype.

Supplemental FIG. 5

Adipose *Hif1a* deficiency induces NEFA release under hypoxic conditions. aP2-*Hif1a*KO adipocytes (black bars) cultured in normoxia (21%O_2) or hypoxia (1%O_2) and stimulated with CL316,243 show increased lipolytic response in hypoxia (n=4/group). Quantification of immunoblots of***)*** basal and CL316,243 stimulated HSL, phosphorylated HSL and perilipin levels ***(A-C)*** (n=3/group) in aP2-*Hif1a*KO adipocytes in hypoxia. Total HSL and perilipin

protein levels are corrected for beta ACTIN (AU), and phosphorylated HSL corrected for total HSL (AU). * $p<0.05$, ***$p<0.001$ comparisons between genotypes.

Supplemental FIG. 6

Adipose *Hif2a* deficiency does not affect lipolysis. ***(A)*** NEFA release in medium of Ap2-*Hif2a* (black bars) adipocytes cultured in normoxia (21% O_2) or hypoxia (1% O_2) and stimulated with CL316,243 show similar lipolytic response to control *Hif2a* (white bars) adipocytes (n=4/group). ***(B)*** Representative immunoblots of basal total HSL levels and quantification graph (n=3/group) in Ap2-*Hif2a* adipocytes in normoxia and hypoxia. ***(C)*** Representative immunoblots of CL316,243 stimulated total HSL levels and quantification graph (n=3/group) in Ap2-*Hif2a* adipocytes in nomoxia and hypoxia. Protein levels are corrected for beta ACTIN levels.

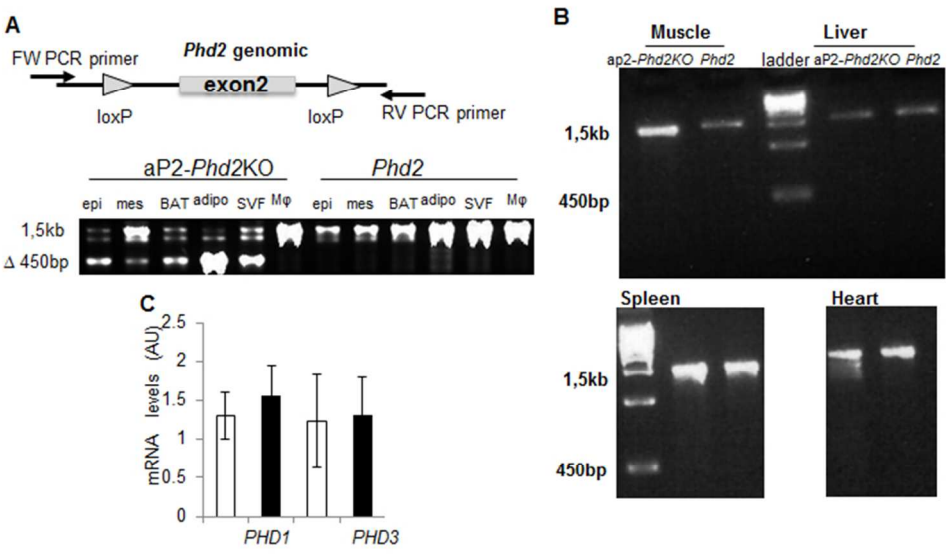

SUPPLEMENTAL FIGURE 1
193x109mm (96 x 96 DPI)

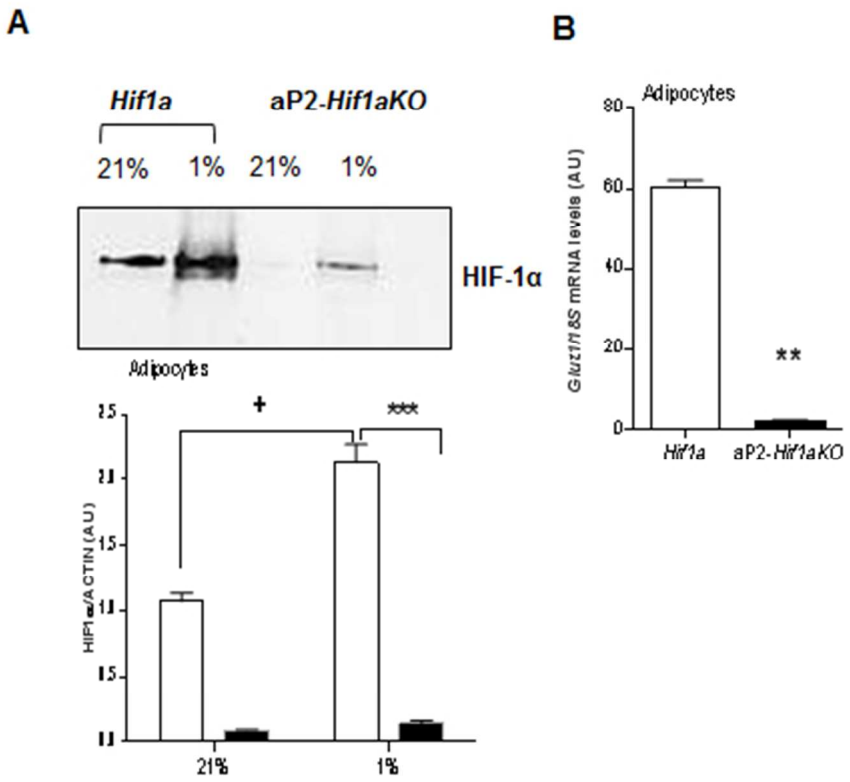

SUPPLEMENTAL FIGURE 2
121x107mm (96 x 96 DPI)

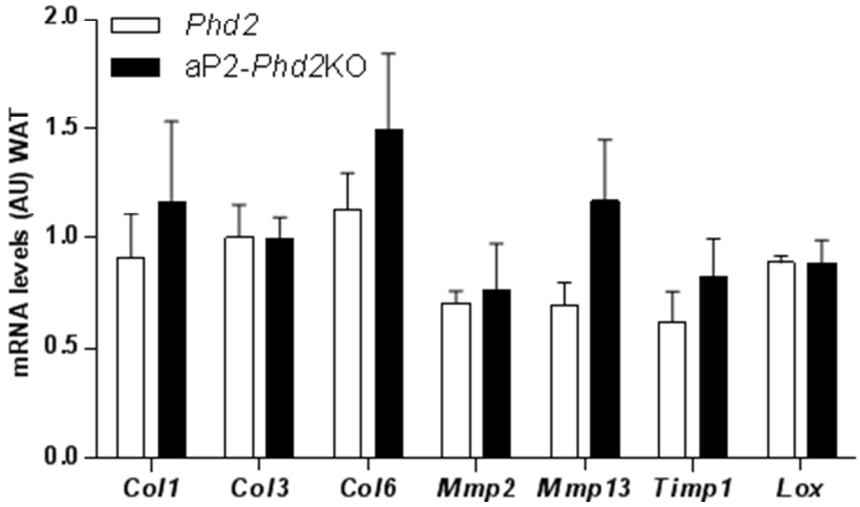

SUPPLEMENTAL FIGURE 3
140x94mm (96 x 96 DPI)

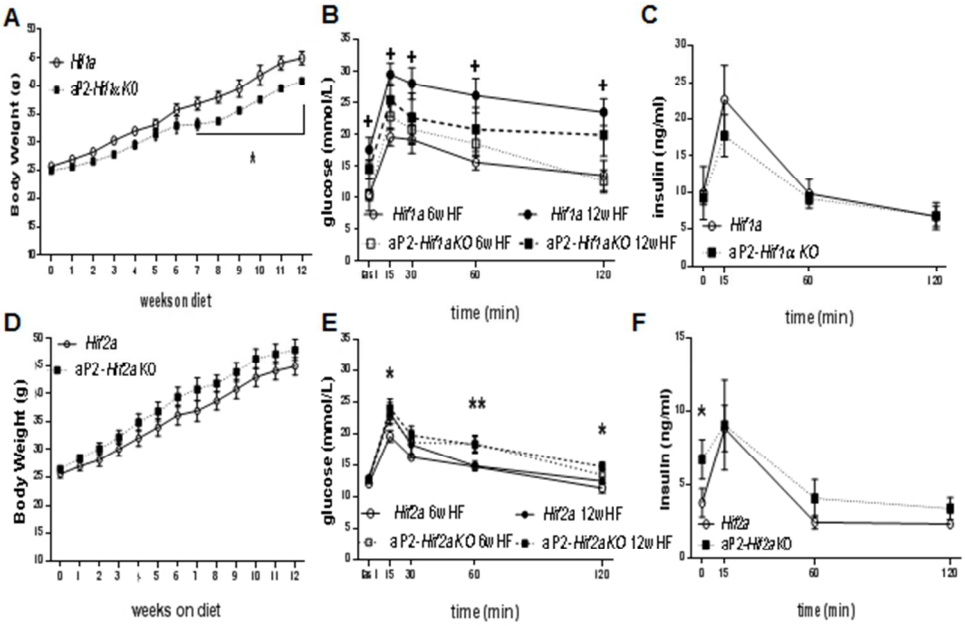

SUPPLEMENTAL FIGURE 4
175x114mm (96 x 96 DPI)

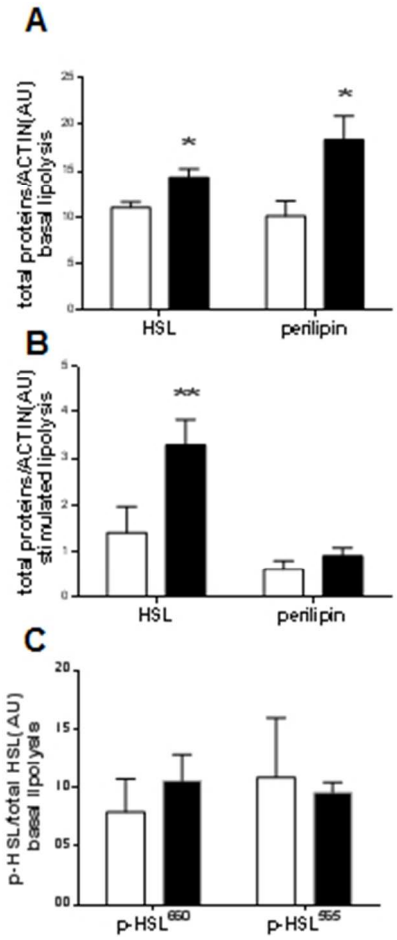

SUPPLEMENTAL FIGURE 5
60x127mm (96 x 96 DPI)

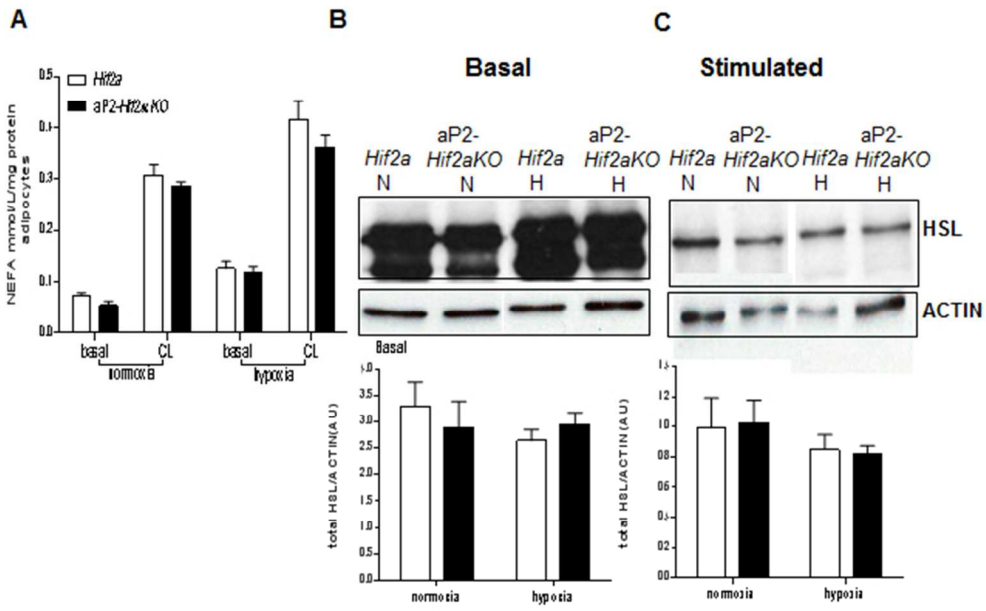

SUPPLEMENTAL FIGURE 6
171x107mm (96 x 96 DPI)